Journal of Non-Crystalline Solids 499 (2018) 208–216

Contents lists available at ScienceDirect

Journal of Non-Crystalline Solids

journal homepage: www.elsevier.com/locate/jnoncrysol

Influence of glass composition on the kinetics of glass etching and frosting in concentrated HF solutions

Nicolas Piret[a,b], Ronny Santoro[a], Loïck Dogot[b], Bastien Barthélemy[b], Eugénie Peyroux[b], Joris Proost[a,*]

[a] Institute of Mechanics, Materials and Civil Egineering (iMMC), Université catholique de Louvain, B-1348 Louvain-la-Neuve, Belgium
[b] AGC Technovation Centre, AGC Glass Europe, B-6041 Gosselies, Belgium

ARTICLE INFO

Keywords:
Glass etching
Glass frosting
Kinetics
Multicomponent glass

ABSTRACT

During etching of a multicomponent glass in concentrated hydrofluoric acid (HF) solutions, a crust can gradually appear on the glass surface, depending on the chemical etching parameters. This crust deposition is the result of the precipitation of hexafluorosilicate anions released by the glass dissolution reaction, with cations coming either from the etching solution or from the glass (like Na^+, K^+ or Ca^{2+}). To understand the impact of this crust on the overall kinetics of both the etching and frosting process, we have studied the dissolution of four types of commercial glass substrates in etching solutions containing various concentrations of HF. The kinetics of the frosting process was investigated by two independent methods: on the one hand the chemical analysis by ICP-OES of the amount of Si dissolved from the glass as a function of time, and on the other hand the measurement of the glass weight loss with time. These two methods showed that the glass etching rate decreases with time as a result of crust formation which gradually becomes more protective. Both methods also indicated that increasing the amount of HF in the etching solution increases the etching rate in a non-linear way, and that the etching rate increases with the alumina content of the glass. A separate chemical analysis of the amount of Si present in the crust also revealed that the amount of HF in the etching solution has an impact on the amount of crust deposited on the glass surface. Finally, we have been able to rationalize all these kinetic data based on a semi-empirical quantitative etching and frosting model, allowing to extract a characteristic dissolution and precipitation constant (K_{diss} and K_{dep}), respectively.

1. Introduction

Using hydrofluoric acid (HF) to etch silica or glass is largely used in different domains. For instance, HF etching can be used for removing the native oxide on Si wafers for micro- or nano-electronic applications, or for chemically polishing a glass surface to remove small surface defects. [1, 2] HF etching can also be used in glass surface micro-machining [3, 4] or in etching glass fibers to produce near-field optical probes [5]. One other notable use of hydrofluoric acid is the production of flat mat or frosted glass surfaces in the glass industry. Even though the latter industrial process is not recent, only a few papers deal with the etching process leading to a frosted glass. [6–8] Indeed, the majority of the articles about silicon or silica wet etching only treat the HF-dissolution step, mostly describing the influence of chemical parameters of the etching bath on the etching rate. [9–13] However, during a glass frosting process, glass dissolution does not occur alone. In that case, it is the formation of a solid crust on the glass surface, precipitating from the combination of glass dissolution products and cations present in the etching solution, that is generally the rate-determining step to get a frosted glass, rather than a blurry transparent glass. Such glass frosting can be described by the following sequence of dissolution and precipitation reactions [8, 14].

$$SiO_{2(s)} + 6HF \rightarrow H_2SiF_6 + 2\,H_2O \quad (1)$$

$$H_2SiF_6 \rightarrow SiF_6^{2-} + 2H^+_{(aq)} \quad (2)$$

$$2M^+ + SiF_6^{2-} \rightleftharpoons M_2SiF_{6\,(s)} \quad (3)$$

Texturing salts like chloride, sulfate or bifluoride (NH_4HF_2, i.e. ammonium bifluoride (ABF), or KHF_2, i.e. potassium bifluoride (KBF)), are usually added to the etching solution to form a texturing crust that creates microstructures on the glass surface during the frosting process. The role of these salts is, on the one hand to generate HF and HF_2^- species in situ that will dissolve the glass, and on the other hand to

* Corresponding author.
E-mail address: joris.proost@uclouvain.be (J. Proost).

https://doi.org/10.1016/j.jnoncrysol.2018.07.030
Received 1 June 2018; Received in revised form 13 July 2018; Accepted 14 July 2018

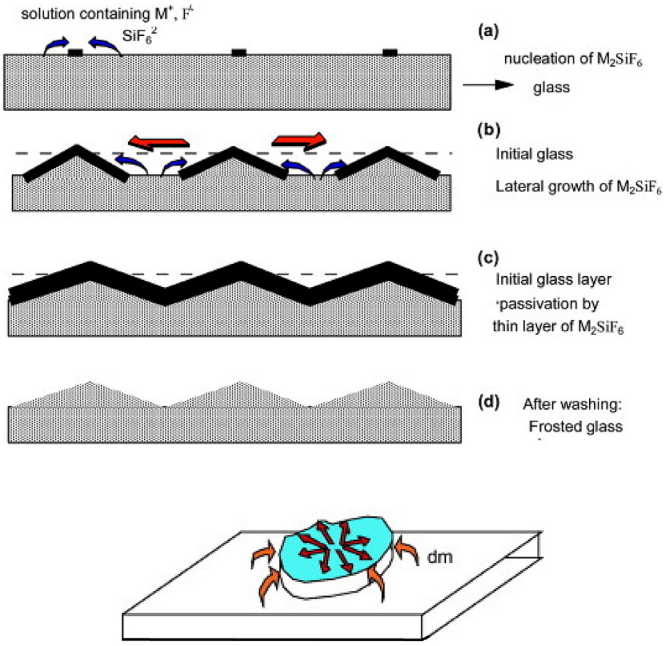

Fig. 1. (top) Schematic illustration of the different steps involved in crust formation and (lateral) growth, leading after washing of the crust to a textured glass surface; (bottom) mechanistic picture of the dissolution and passivation mechanism used in the kinetic modeling, leading to the basic constitutive Eq. (6). Both illustrations are taken from ref. [7].

bring an important amount of cations in solution that will combine with the hexafluorosilicate anions generated during the glass dissolution step. The texturing of the glass surface originates from the fact that the crust formation is a gradual, progressive process, as proposed originally by Barboux et al. and illustrated schematically in Fig. 1 [7]. At the beginning of crust growth (Fig. 1(a)), only some places on the glass surface are protected by nuclei of precipitating salts, leaving unprotected glass exposed to dissolution by the etching solution. As the crust is growing laterally (Fig. 1(b)), less unprotected glass surface is available to be dissolved, until the full glass surface is covered by a crust thick enough to fully inhibit further glass dissolution (Fig. 1(c)). As a result, glass areas covered by initial nuclei of crust will morphologically remain as higher points on the surface, while areas covered only in a later stage by the crust will correspond to lower points, thus generating a microroughness on the glass surface (Fig. 1(d)). It is important to realize that in the above described etching and frosting sequence, crust formation is assumed to occur as the 2-dimensional, lateral growth of a passivation layer with a constant thickness. This has been illustrated by the bottom picture in Fig. 1 as well.

Industrially, a wide range of commercial glass compositions exists. The compositional choice will depend on mandatory specifications of the final application of the glass, such as color, energetic properties, optical properties, mechanical resistance or aesthetics. Besides the major component silica, other oxide components are usually incorporated into the silica glass network as well, including Na_2O, CaO, K_2O, Fe_2O_3, Al_2O_3, MgO or TiO_2. These additional oxides interact with silica during the glass formation process and influence the silica network to give the glass its specific features. These oxides can be separated in two groups: network-modifying oxides and network-forming oxides. Due to presence of these oxides in the glass network, multicomponent glasses have been reported to have a dissolution rate that is more than one order of magnitude larger than that of vitreous SiO_2 [12].

Network-modifying oxides like Na_2O, K_2O or CaO are incorporated in the silica matrix by breaking a siloxane bond and forming non-bridging oxygens by the following reaction:

$$Na_2O + \equiv Si - O - Si \equiv \rightarrow 2 \equiv SiO^{-} \bullet Na^{+} \quad (4)$$

The presence of these broken bonds then strongly increases the etching rate of the glass. As the chemical bond between the silica matrix and cations from the network-modifying oxides is ionic, cations are quite mobile inside the silica matrix. Spierings et al. [12] have suggested that, in aqueous solutions like HF etchants, these cations (mono or bivalent) are leached out of the glass and can be replaced by H_3O^+ ions, thus forming silanol groups ≡Si-OH. As a result of this leaching and ion exchange, a hydrated silica film (approximately 1 μm thick) is formed and precedes the dissolution of the glass in the HF etchant. Fluorine species also diffuse into this hydrated layer and attack Si-O-Si bonds present in this layer.

Network-forming oxides can either be incorporated into the silicate network structure, or form their own separate network that can be mixed with the silicate network. For example, when a network-forming oxide A_xO_y is added to SiO_2, -Si-O-A- and -A-O-A- bonds are formed. Depending on the strength of the A-O chemical bond and its own breakage mechanism, the presence of network-forming oxides can either increase or decrease the etching rate of the glass. Working with aluminosilicate glass, Saito et al. showed that not only alkali or alkali earth metal oxide but also alumina can be leached out in HF solutions, leading to an increase in etching rate with Al_2O_3 content [20, 21].

As multicomponent glasses can contain both network-modifying and network-forming oxides, the influence of the glass composition on the etching rate can be quite complex. Spierings suggested that, for multicomponent glass, the etch rate is predominately determined by two factors: the connectivity (or the degree of linkage) of the silicate-based network, and the concentration of SiO_2 in the glass [14–16]. The following dissolution mechanism of a multicomponent glass has therefore been proposed [14, 17–19]:

- adsorption of the active fluorine species on the glass surface;
- leaching of the alkali and alkaline earth cations to form a porous layer (in the case of network-modifying oxides);
- fast rupture of the X-O-Si bonds (in the case of network-forming oxides with X being B, Al or Zn), and leaching of these species;
- breaking of the Si-O-Si bonds at the glass-solution interface and also further away from the interface, through diffusion of HF molecules and HF_2^- ions into the leached surface layer;
- desorption of fluorosilicates.

Finally, cations coming from other oxides present in the glass are being leached out during dissolution in HF, and can combine with hexafluorosilicate anions also formed by the SiO_2 network dissolution. They form a crust on the glass surface even if no texturing salts are added to the etching solution.

The objective of the current paper is to study the influence of specific industrially relevant glass compositions on the glass etching rate for various HF concentrations. Contrary to all previous publications, the crust appearing during the texturing process was analyzed chemically as well, and the influence of its appearance on the glass dissolution rate has been investigated independently. The two used methods were the chemical analysis by ICP-OES of the amount of Si dissolved from the glass as a function of time, and the measurement of the glass weight loss with time. Then, a dissolution/precipitation model from the literature has been used to fit our experimental data and its use and limits are discussed. Also, a new parameter is proposed to characterize the crust formation process.

2. Material and methods

Four kinds of commercial glass substrates have been compared. Table 1 shows the composition of these glasses, as well as their gravimetric density. This glass series was specifically chosen in order to have various amounts of alumina (Al_2O_3), the latter already having been

Table 1
Glass compositions considered in the present study.

Glass	Density (g/cm^3)	Composition (wt%)								
		SiO_2	Al_2O_3	CaO	K_2O	Na_2O	Fe_2O_3	SO_3	TiO_2	MgO
A	2.490 ± 0.005	71.64	1.352	7.88	0.236	13.91	0.104	0.326	0.055	4.45
B	2.478 ± 0.005	66.40	5.772	1.06	1.042	15.74	0.0193	0.268	0.024	9.60
C	2.481 ± 0.007	60.11	13.241	0.18	5.970	12.60	0.0198	0.051	0.017	6.69
D	2.471 ± 0.010	61.28	16.907	0.12	0.884	15.34	0.0084	0.066	0.067	5.03

reported in the past to have an influence on the glass etching rate [21]. Prior to etching, all glasses are cleaned twice with a 2 vol% solution of RBS 50 detergent (Chemical Products R. Borghgraef S.A.), rinsed two times with ultrapure water (18.2 MΩ.cm) and dried at room temperature for 30 min.

All etching experiments are done using a horizontal etching cell, and performed on the glass surface which has not been exposed to the tin bath during the float process. In this etching cell, the glass is placed between two stainless steel plates having a central circular opening 9 cm in diameter. The glass and stainless steel plates are sealed by a rigid circular Teflon ring having an internal diameter of 8.4 cm. This kind of cell allows to keep a constant surface area exposed to the etching solution for all experiments. HF solutions are prepared from a commercial 40 wt% HF solution (NORMAPUR analytical grade, VWR Chemicals), and mixed with ultrapure water to give different HF concentrations ranging from 0.5 to 5 M. Also, the volume of the etching solution is kept constant at 25 ml to exclude any influence of the solution volume on the kinetics of the dissolution and the crust formation process.

The kinetics of the frosting process was investigated by two independent methods: on the one hand the chemical analysis of the amount of Si dissolved from the glass by Inductively Coupled Plasma Optical Emission Spectroscopy (ICP-OES), and on the other hand the measurement of the glass weight loss for different etching times. In the first method, two Si fractions were separately collected and analyzed: the etching fraction is the amount of Si dissolved in the etching solution and collected as such after the etching, while the rinsing fraction represents the amount of Si in the crust that appeared on the glass surface, as obtained after being rinsed with ultrapure water. In the second method, the glass is weighed before and after etching and rinsing, respectively. In both methods, a separate glass sample is used for one etching duration and one HF concentration only.

The crust was also collected as a solid dry powder. This was done by removing the remaining etching solution in the cell after etching, and rinsing the wet crust three times with 20 ml of acetone (AnalaR NORMAPUR analytical grade, VWR Chemicals) while it was still attached to the glass surface. The glass sample with the crust on it was then dried on a heating plate for 20 min at 40 °C, and weighed before and after removing the crust.

3. Results

Before going into detail in our quantitative kinetic data, Table 2 represents a summary of qualitative visual observations of the crust appearing on the glass for all the etching experiments. It can be seen that the crust appears faster and for less concentrated HF solutions in the following order: Glass D, Glass C, Glass B and Glass A. This already indicates that the composition of the glass clearly has a significant influence on the etching and frosting process, and this trend seems to correlate with an increasing amount of alumina in the glass.

3.1. Etching and frosting kinetics from chemical analysis of Si fractions by ICP-OES

A typical result of the total amount of etched Si as a function of time is shown in Fig. 2. First of all, it is clear that increasing the amount of HF in the etching solution increases the etching rate because more glass will be dissolved at higher HF concentrations for each etching time.

Table 2
Visual observation of all glasses and their crust formation, after etching for different times in various HF concentrations. Green = no crust observed on the glass surface; yellow = some crystals observed on the glass surface; red = a crust is observed on the glass surface.

	HF Conc.	Etching time (s)							
	(M)	30	60	90	120	180	240	300	420
Glass A	0.5								
	1								
	2								
	5								
Glass B	0.5								
	1								
	2								
	5								
Glass C	0.5								
	1								
	2								
	5								
Glass D	0.5								
	1								
	2								
	5								

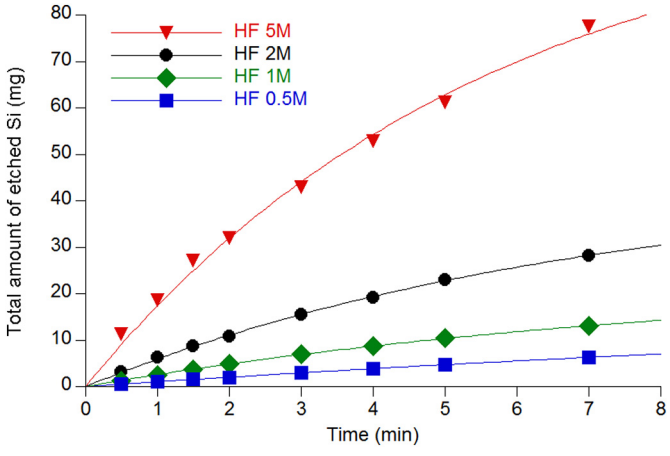

Fig. 2. Total amount of etched Si (Glass D) as a function of etching time for different HF concentrations. Lines are quantitative fits using the dissolution/precipitation model of Barboux et al. [7] according to Eq. (5).

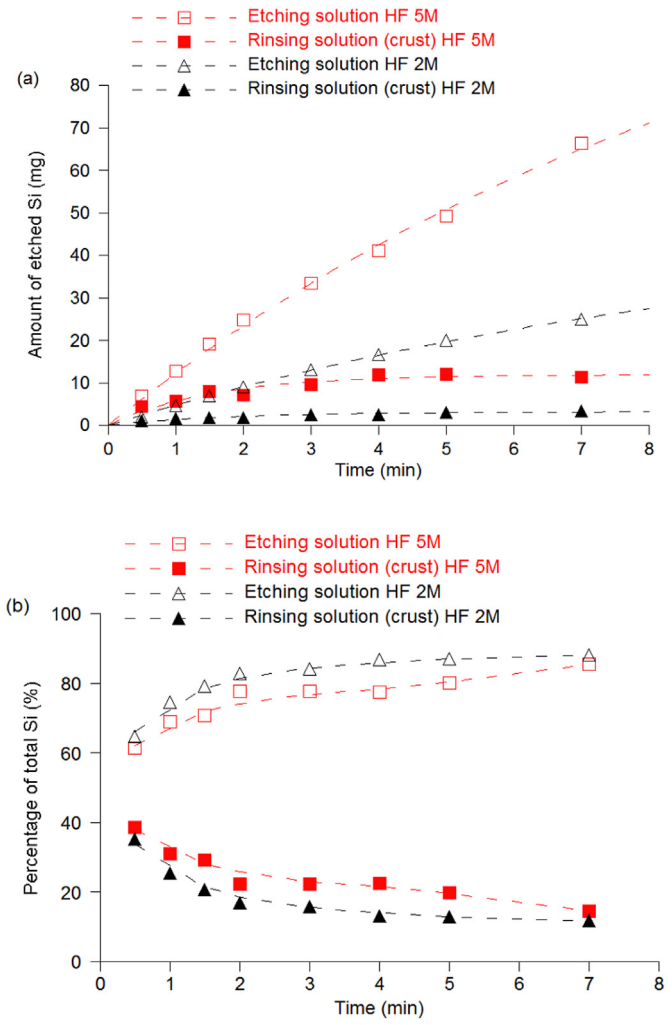

Fig. 3. Amount of etched Si (Glass D) in each of the etching and rinsing fractions as a function of etching time for a 2 M and a 5 M HF etching solution, expressed either in absolute (a) or in relative (b) terms. Dotted lines are guides to the eye only.

Also, these data indicate that the etching rate of the glass is not constant with time. Indeed, it decreases because of the gradual appearance of a crust on the glass surface during etching. This crust has indeed a protective effect which gradually slows down the etching kinetics, resulting in curves that tend towards a plateau.

As the total amount of etched Si is the sum of the Si collected in both the etching and rinsing fractions, Fig. 3 represents a typical result of the amount of Si present in each of these two fractions separately as a function of time. For both fractions, expressed either in absolute (a) or in relative terms (b), it can be seen that the etching rate of Si is not constant with the time, and that the major part of Si can be found in the etching fraction. Also, increasing the amount of HF in the etching solution seems to increase the amount of Si present in the crust both in absolute amount and in relative terms, indicating that the crust will grow thicker with higher HF concentrations in the etching solution. However, for both HF concentrations, the relative amount of Si in the crust fraction decreases with time, indicating that its passivating effect is most pronounced in the early stages of the frosting process.

3.2. Etching kinetics from glass weight loss measurements

A characteristic result of glass weight loss as a function of etching time is presented in Fig. 4. These data show essentially the same trends as those observed for the total amount of etched Si: an increase of the etching rate when increasing the HF concentration in the etching solution, and a decrease in etching rate with time because of the gradual appearance of a protective crust on the glass surface during etching.

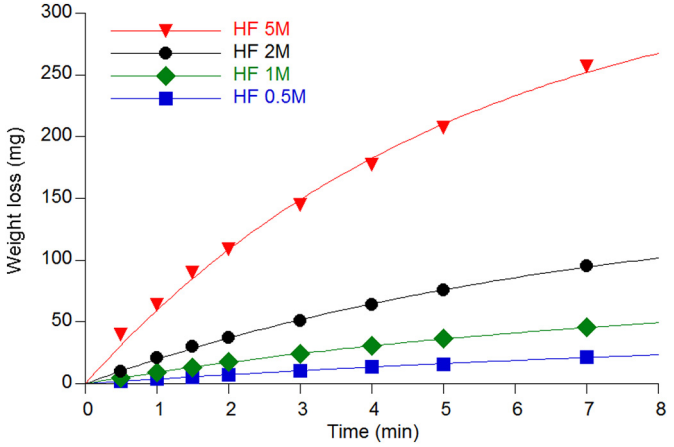

Fig. 4. Weight loss of Glass D as a function of etching time for different HF concentrations. Lines are quantitative fits using the dissolution/precipitation model of Barboux et al. [7] according to Eq. (5).

4. Discussion

4.1. Dissolution/precipitation model

The glass weight loss data of Fig. 4 (and indirectly also the data of Fig. 2) can be fitted using the dissolution/precipitation model developed by Barboux et al. [7]. This model describes the time evolution of the glass weight loss by the following equation:

$$m_g(t) = m_{max} \cdot [1 - exp(-K_{diss} \cdot K_{dep} \cdot t)] \quad (5)$$

It allows to extract two fundamental kinetic parameters from each curve: m_{max}, corresponding to the maximum amount of glass that can be dissolved, and the product of a so-called dissolution constant K_{diss} and a deposition or crusting constant K_{dep}. As to the latter, Barboux et al. showed experimentally in ref. [7] that there seems to exist a linear relationship between the mass of the precipitated crust and the glass weight loss dm. This was formalized as:

$$S \cdot d\theta = K_{dep} \cdot dm \quad (6)$$

S being the exposed glass surface, and θ its fraction being covered by the crust. Eq. (6) is also a direct result of the schematic picture of Fig. 1, imagining crust formation as the 2-dimensional, lateral growth of a passivation layer with a constant thickness.

As to K_{diss}, this parameter naturally arises from the fact that the fraction of glass dissolved during an increment of time dt depends on the amount of glass surface not being covered by the passivating crust layer [7]:

$$dm = K_{diss} \cdot (1 - \theta) \cdot S \cdot dt \quad (7)$$

By inserting Eq. (6) into Eq. (7), one then arrives at Barboux's macroscopic kinetic Expression (5).

4.2. Validation of the model to our experimental data

In order to validate the applicability of Barboux's dissolution/precipitation model to our own glass weight loss data, Fig. 5 represents, as in Barboux's paper [7], the mass of the crust per unit glass surface area as a function of the glass weight loss, expressed as an equivalent thickness (i.e. the thickness of glass dissolved). The latter is obtained by dividing the weight loss by the density of the glass and its surface area exposed to the etching solution. This was compared in Fig. 5(a) for all

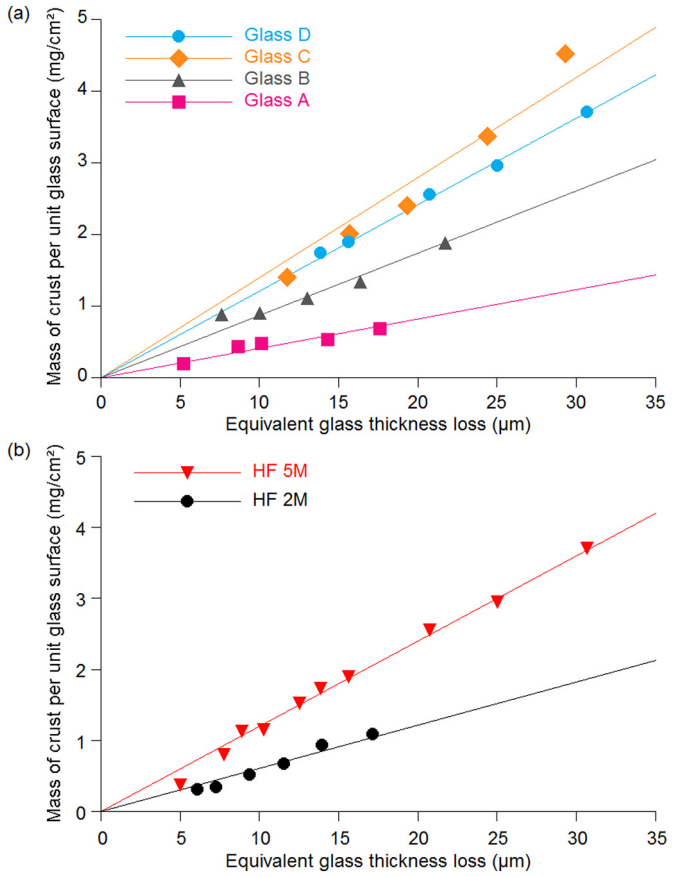

Fig. 5. Mass of the crust appearing on the glass surface during etching as a function of the equivalent thickness of glass dissolved, (a) for etching of all glass compositions in a 5 M HF solution, and (b) for the etching of glass D in different HF concentrations.

glass compositions etched in a 5 M HF solution, and in Fig. 5(b) for glass D etched in different HF concentrations.

The linear relationship claimed by Barboux is clearly also present for our own different glass compositions and their corresponding crusts. However, contrary to Barboux' findings, the slope of the linear fits in Fig. 5, which is seen from Eq. (6) to be directly proportional to K_{dep}, seems to depend both on the composition of the crust (which in turn can be expected to depend on the glass composition), and also on the HF concentration. This latter trend can be linked to observations reported by Frayret et al., where the solubility limit of hexafluorosilicate salts was reported to be modified by the HF concentration of the solution [22]. It could also be explained by the fact that, with higher HF concentration, more glass is dissolved, so that locally more cations released from the glass can combine with more SiF_6^{--} anions produced by the dissolution of the glass. Near the glass surface, the solubility limit of produced salts is quickly reached and more crust can precipitate. When the HF concentration is lower, the dissolution process is slower and less cations and SiF_6^{--} anions are released in the near neighborhood of the glass surface. As a result, these ions can diffuse further away from the glass surface before the solubility limit is reached. This results in a lesser amount of crust for the same amount of glass dissolved, and therefore also a smaller slope. It can also be noted that the degree of texturing of the glass after etching does not seem to have an impact on the observed linear relationship. Indeed, in the work of Barboux et al. heavily textured glass surfaces were obtained, while in our case only a few microstructures were observed on the glass surface after etching.

4.3. Determination of the dissolution and deposition constants K_{diss} and K_{dep}

Since fitting of our experimental data with the precipitation/dissolution model of Barboux et al. only allows to extract the product of the dissolution and deposition constants $K_{diss}{\cdot}K_{dep}$, an additional analysis is still needed to obtain each constant independently. The value of the deposition constant K_{dep} can be found from Eq. (6), which can be rewritten as:

$$K_{dep} = \frac{S{\bullet}d\theta}{dm} \tag{8}$$

In this expression, the covering ratio θ can be obtained by inserting Eq. (7) into Eq. (6):

$$S{\bullet}d\theta = K_{diss}{\bullet}K_{dep}{\bullet}(1-\theta){\bullet}S{\bullet}dt \tag{9}$$

Then, Eq. (9) can be written as:

$$\frac{d\theta}{(1-\theta)} = K_{diss}{\bullet}K_{dep}{\bullet}dt \tag{10}$$

which, after integration, gives the following expression of the covering ratio as a function of time:

$$\theta(t) = 1 - exp(-K_{diss}{\bullet}K_{dep}{\bullet}t) \tag{11}$$

Comparing Eq. (11) and Eq. (5) then indicates that the time evolution of the covering ratio θ can be found by simply dividing the measured glass weight loss m(t) by the value of m_{max} obtained previously from a fit to the experimental data with the macroscopic dissolution/precipitation model.

Thus, by expressing the evolution of the surface area covered by the crust $S{\cdot}\theta$ as a function of the amount of dissolved glass m, as presented in Fig. 6, the deposition constant K_{dep} constant can be calculated, according to Eq. (8), as the slope of the linear fits.

Finally, the value of the dissolution constant K_{diss} can then simply be obtained by dividing the product $K_{diss}.K_{dep}$, obtained from the Barboux model, by the deposition constant K_{dep} calculated independently as explained above.

Fig. 7 presents the dependency of the dissolution constant K_{diss} and the deposition constant K_{dep} on HF concentration for different glass compositions. The non-linear increase observed in the evolution of the dissolution constant K_{diss} will be discussed later with the analysis of the initial etching rates (see Section 4.4). For the deposition constant K_{dep}, a non-linear decrease is observed as a function of HF concentration for all glass compositions. Moreover, all curves seem to follow one single master curve, indicating that K_{dep} is not affected by the glass composition. At first sight, the latter observation might seem to be in contradiction with the observation presented previously in Fig. 5. Indeed, on the one hand, the increase in slope with HF concentration in

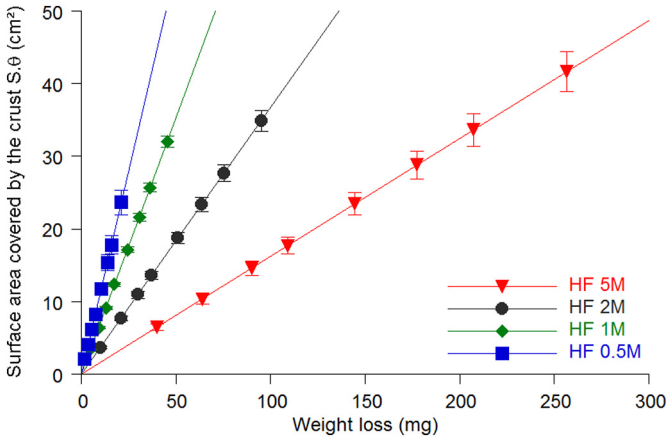

Fig. 6. Surface area covered by the crust ($S.\theta$) as a function of weight loss m. Data are for etching of glass D in different HF concentrations.

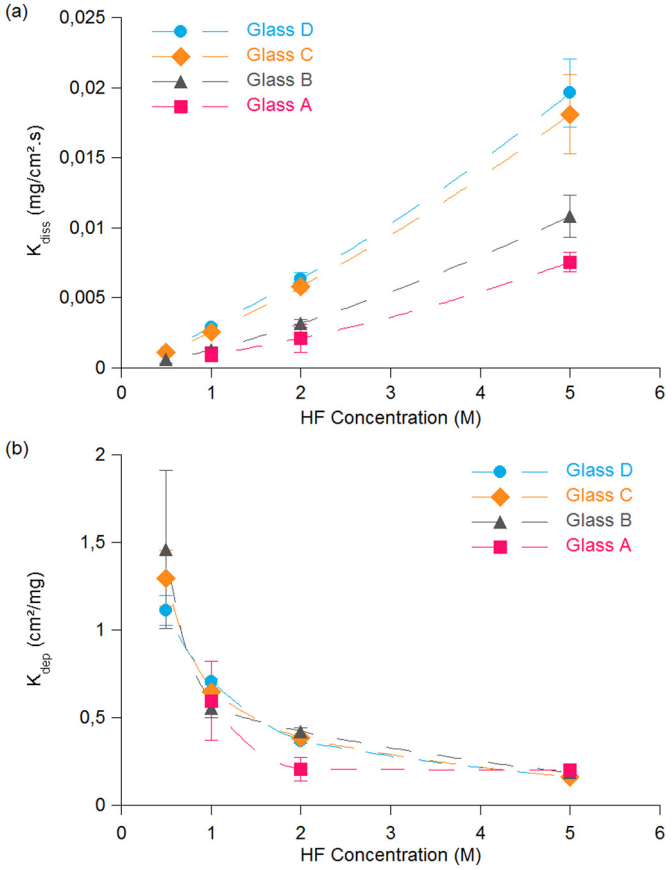

Fig. 7. Dissolution constant K_{diss} (a) and deposition constant K_{dep} (b) as a function of HF concentration for all glass compositions. Dotted lines are guides to the eye only.

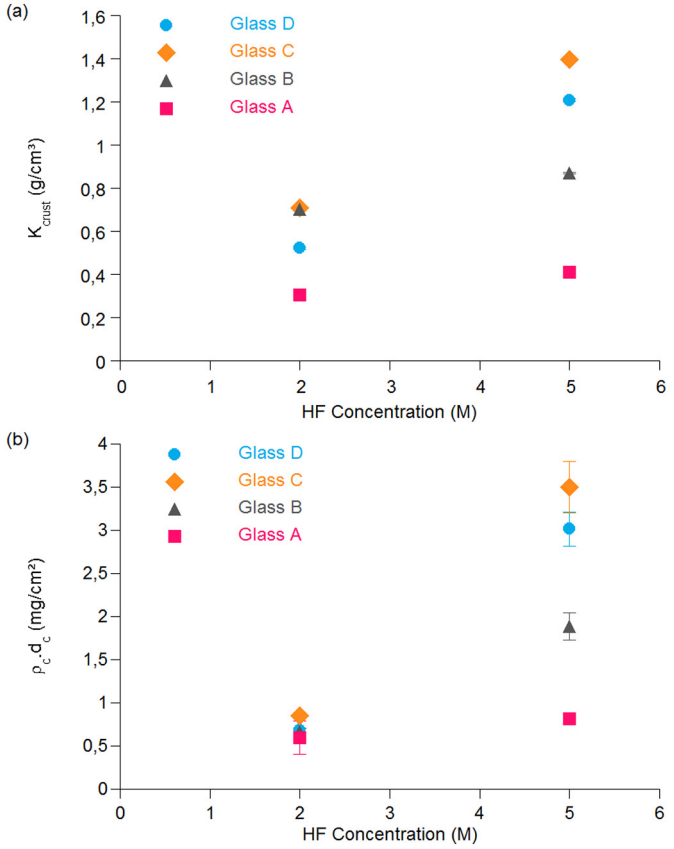

Fig. 8. Evolution of K_{crust} (a) and the surface density of the crust $\rho_c.d_c$ (b) as a function of HF concentration for all glass compositions.

Fig. 5(b) indicates that more crust is produced per unit glass surface at higher HF concentration, while in Fig. 7(b) the decrease of K_{dep} with the HF concentration implies that less surface area is covered by the crust per gram of glass dissolved at higher HF concentrations. This apparent contradiction results from the fact that the definition of K_{dep} is based only on the surface area of crust, and therefore does not take into account its thickness or mass density.

As a matter of fact, the slope of the linear fits in Fig. 5 can be linked directly to the deposition constant K_{dep}. Indeed, the mathematical expression of the observed linear fit in Fig. 5 is

$$\frac{m_c}{S} = K_{crust} \bullet d_g \tag{12}$$

where m_c is the mass of the crust, S the total exposed area, K_{crust} the slope of the linear fit and d_g the equivalent glass thickness loss. The latter can be further expressed as:

$$d_g = \frac{m_g}{\rho_g \bullet S} \tag{13}$$

where m_g is the mass of the glass and ρ_g the glass density. Inserting Eq. (13) into Eq. (12) then gives:

$$\frac{m_c}{S} = K_{crust} \bullet \frac{m_g}{\rho_g \bullet S} \tag{14}$$

The mass of the crust m_c in Eq. (14) can also be expressed as the product of the crust density ρ_c, the surface of the crust S_c and its thickness d_c:

$$\frac{\rho_c \bullet S_c \bullet d_c}{S} = K_{crust} \bullet \frac{m_g}{\rho_g \bullet S} \tag{15}$$

Since the covering ratio θ is defined as the surface of crust S_c divided by the total exposed surface S ($\theta = S_c / S$), Eq. (15) can also be written in the following form:

$$m_g \bullet \frac{K_{crust}}{\rho_g \bullet \rho_c \bullet d_c} = \theta \bullet S \tag{16}$$

Comparing Eq. (6) and Eq. (16) reveals that the link between K_{crust} and K_{dep} is:

$$K_{crust} = K_{dep} \bullet (\rho_g \bullet \rho_c \bullet d_c) \tag{17}$$

Thus, compared to K_{dep}, K_{crust} takes additionally into account the densities of both the glass and the crust, as well as its thickness. As a result, by dividing K_{crust} and K_{dep}, we can extract a new parameter to characterize the crust, namely the product of the crust density and its thickness ($\rho_c.d_c$), which represents the crust surface density. As an example, Fig. 8(a) presents values of K_{crust} as a function of HF concentration for all glass compositions (i.e. the slopes of the linear fits in Fig. 5), while Fig. 8(b) shows values of the corresponding surface densities $\rho_c.d_c$ of the crust.

For reasons already discussed in Section 4.2, the constant K_{crust} is clearly affected by the glass composition and increases with the HF concentration of the etching solution. Indeed, for all glass compositions, a higher HF concentration results in an increase in the amount of crust formed per unit volume of dissolved glass. At the same time however, the surface density of the crust also increases with HF concentration, indicating that a higher HF concentration also gives a denser and/or thicker crust. The magnitude of this increase seems to strongly depend on the composition of the glass. Since according to Eq. (17)K_{dep} is proportional to the ratio of K_{crust} and $\rho_c.d_c$, its dependency on the glass composition is much less visible.

It is important to realize that in the above kinetic modeling, the

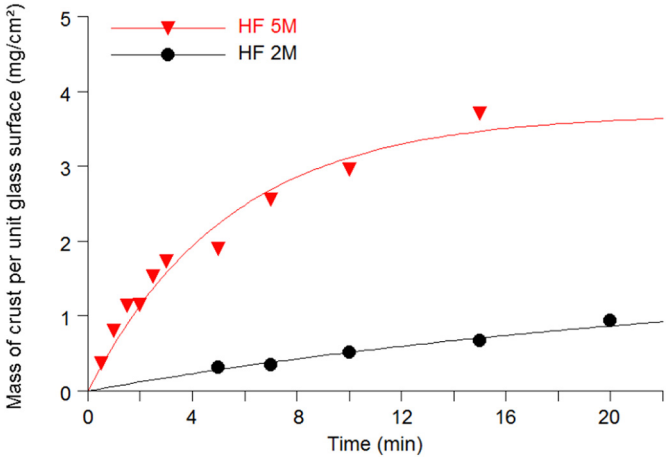

Fig. 9. Evolution of the mass of the crust as a function of time for glass D in 2 M and 5 M HF etching solutions. Lines are quantitative fits according to Eq. (20).

thickness of the passivating crust d_c is being considered to be independent of time. This was already stated explicitly above as a fundamental assumption to validate the basic constitutive Eq. (6). It also follows directly from Eq. (16), which, since the time dependencies of m_g (Eq. 5) and θ (Eq. 11)) cancel out, can be rewritten as:

$$d_c = \frac{K_{crust} \cdot m_{max}}{\rho_g \cdot \rho_c \cdot S} \tag{18}$$

Nonetheless, the kinetics of crust growth can still be analyzed through the evolution of the mass of the crust as a function of the time. This is shown in Fig. 9 for the etching of glass D in 2 M and 5 M HF solutions. Note that due to practical limitations, the mass of the crust could not be determined for etching times below 5 min in 2 M HF solutions Indeed, for these times, the amount of crust formed on the glass surface is insufficient to be separated following our experimental procedure. For the same reason, no crust data could be obtained for the 0.5 and 1 M HF solutions.

It can be observed that the mass of the crust is increasing with time in a non-linear way, rather similarly as was observed for the time evolution of the mass loss of etched glass in Fig. 4. As a matter of fact, an equation similar to Eq. (5) can be derived to describe the time evolution of the mass of the crust. Indeed, starting from the basic definition of the covering ratio $\theta(t) = S_c(t)/S$, with $S_c(t)$ being the surface area covered by the crust and S being the total exposed glass surface, it can be written that

$$\theta(t) = \frac{S_c(t) \cdot d_c \cdot \rho_c}{S \cdot d_c \cdot \rho_c} = \frac{m_c(t)}{m_{c,max}} \tag{19}$$

where d_c is the thickness of the crust, ρ_c its density, $m_c(t)$ the mass of crust evolving with time, and $m_{c,max}$ the maximum amount of crust mass that will be formed at full surface coverage. From Eq. (19), the time evolution of the mass of the crust with time is then given by

$$m_c(t) = m_{c,max} \cdot \theta(t) = m_{c,max} \cdot [1 - exp(-K_{diss} \cdot K_{dep} \cdot t)] \tag{20}$$

where the full expression of $\theta(t)$ has been taken from Eq. (11).

As already anticipated before, the original expression from the model of Barboux for the time evolution of the mass loss of the etched glass (Eq. (5)) can also be used to describe the mass of the crust appearing during the frosting process (Eq. (21)). The fundamental reason for this is that the mass of the crust and the mass loss of the etched glass are directly linked, as already evidenced in Fig. 5. Moreover, the observed linearity when expressing the crust mass values as a function of the equivalent glass thickness loss indicates that the crust thickness d_c can indeed be considered to be constant with time. Indeed, as a result of the observations in Fig. 5, the following proportionality could be written (cfr. Eq. (14)):

$$m_c = \frac{K_{crust} \cdot m_g}{\rho_g} \tag{21}$$

If the crust thickness d_c was not constant with the time, then, according to Eq. (17), K_{crust} would not be constant with the time neither, and therefore the observed proportionality between the mass of the crust and the mass loss of etched glass shown in Fig. 5 and described by Eq. (21) would not have been observed. In this respect, it is also quantitatively reassuring that very similar values for the fitting parameters of the 5 M solution are obtained when applying Eq. (20) to the crust growth data in Fig. 9 ($K_{diss} \cdot K_{dep} = 0.19 \pm 0.03\ min^{-1}$; $\rho_c \cdot d_c = 3.7 \pm 0.03\ mg/cm^2$) as when applying Eq. (5) to the corresponding glass weight loss data of Fig. 4 ($K_{diss} \cdot K_{dep} = 0.19 \pm 0.01\ min^{-1}$; $\rho_c \cdot d_c = 3.1 \pm 0.02\ mg/cm^2$).

4.4. Effect of glass composition on the initial etching rate

In order to extract some other quantitative kinetic dissolution data from the glass weight loss curves, the initial etching rate can be taken as a relevant representative point of comparison because, at time zero, there is no crust formed yet. This initial etching rate can be extracted from the slope at the origin of the glass weight loss vs. time data in Fig. 4. This slope can most easily be obtained by taking the derivative of Eq. (5)

$$\frac{dm(t)}{dt} = m_{max} \cdot K_{diss} \cdot K_{dep} \cdot (e^{-K_{diss} K_{dep} t}) \tag{22}$$

and evaluating it at $t = 0$:

$$\left(\frac{dm}{dt}\right)_{t=0} = m_{max} \cdot K_{diss} \cdot K_{dep} \tag{23}$$

Initial etching rates calculated as such are expressed as a function of HF concentration in Fig. 10. A non-linear increase of the initial etching rate can be observed when increasing the HF concentration. This non-linearity can be attributed to the increasing presence of species more reactive than hydrofluoric acid, like HF_2^- or H_2F_2, when the HF concentration of the solution increases [5, 12, 18]. The same trend has also been reported by Iliescu et al. for the etching of Pyrex (borosilicate) glass [23, 24].

Note that the evolution with HF concentration of these initial etching rates is exactly the same as the one for the dissolution constant

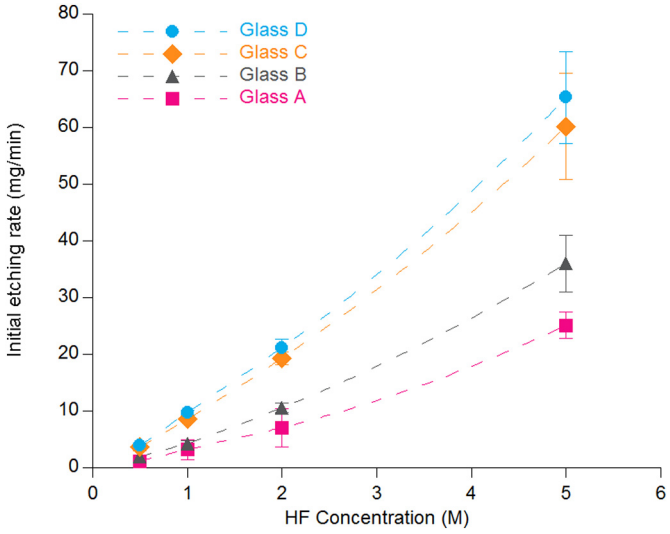

Fig. 10. Initial etching rates, calculated from weight loss measurements (Eq. 24), as a function of HF concentration for all glass compositions. Dotted lines are guides to the eye only.

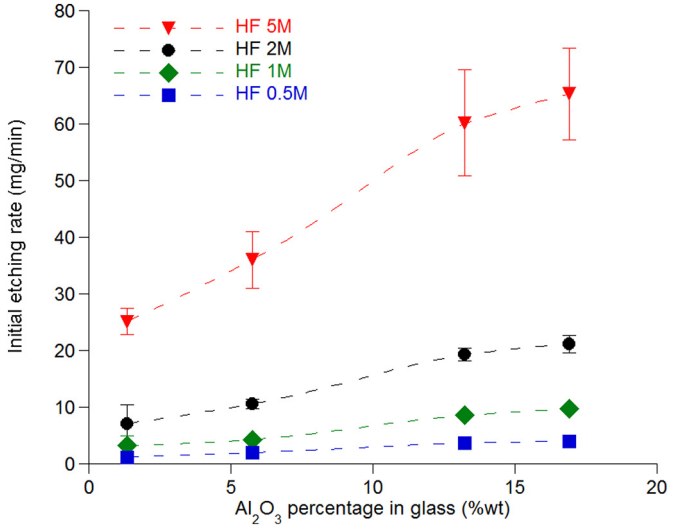

Fig. 11. Initial etching rates as a function of alumina content. Dotted lines are guides to the eye only.

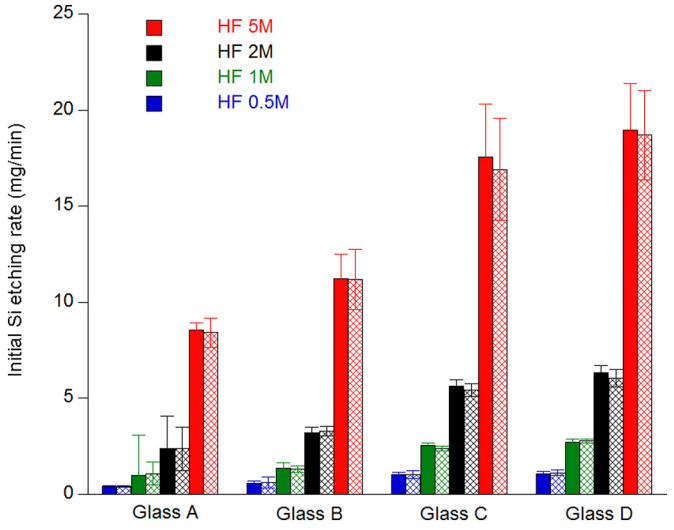

Fig. 12. Comparison of initial silicon etching rates, as obtained independently from the total amount of etched silicon by ICP-OES (solid bars), and from glass weight loss measurements converted into initial Si etching rate using the glass composition (striped bars).

K_{diss} shown previously in Fig. 7(a). As a matter of fact, careful analysis reveals that the value of K_{diss} can simply be obtained by dividing the initial etching rate by the total exposed surface area S of the glass:

$$\left(\frac{dm}{dt}\right)_{t=0} = m_{max} \cdot K_{diss} \cdot K_{dep} = K_{diss} \cdot S \quad (24)$$

The above observation therefore also implies that

$$S = m_{max} \cdot K_{dep} \quad (25)$$

By definition, S is the total surface area of glass exposed, so this is the maximum surface that can be covered by the crust when the frosting process is complete (i.e. when time tends to infinity). At that same time, the value of m_{max} corresponds to the maximum amount of glass that can be dissolved. Since the units of the deposition constant K_{dep} are cm^2 of crust per g of dissolved glass, the product of K_{dep} and m_{max} thus gives the maximum amount of surface that can be covered by the crust. The latter simply corresponds to the total surface area S of glass exposed, because if the frosting is complete, all the exposed glass surface is covered by the crust. This demonstrates the validity of Eqs. (24) and (25). As a result, an alternative method in order to separate the deposition and dissolution constants consists in:

- first obtaining the values of m_{max} and the product $K_{diss}.K_{dep}$ from fitting the glass weight loss data to the Barboux model (Eq. 5);
- calculating, based on these 2 fitting parameters, the value of the initial etching rate according to Eq. (24);
- calculating the value of the dissolution constant K_{diss} by diving the initial etching rate by the total exposed surface area S;
- calculating the value of the deposition constant K_{dep} either by dividing the product $K_{diss}.K_{dep}$ by K_{diss}, or based on the value of m_{max} in Eq. (25);

The initial etching rates can also be expressed as a function of the alumina (Al_2O_3) content of the glass. As seen in Fig. 11, the etching rate increases with the amount of alumina for all HF concentrations. However, as all tested glass contains other oxide compounds besides silica and alumina as well (cfr. Table 1), the combined effect of these oxides cannot be excluded.

Finally, Fig. 12 compares the initial etching rates obtained from glass weight loss measurements, converted into initial silicon etching rates using the glass composition of each glass series, to the ones calculated from the total amount of dissolved silicon, as measured by ICP-OES. For the latter, the silicon content present in both the etching and rinsing fractions were added. No statistically significant differences are observed between the 2 independently obtained Si etching rates. This claim is based on hypothesis testing using a so-called Student t-test [25], with a one-sided significance level α of 10%. As a result, the kinetic trends presented in Fig. 10 and Fig. 11 can be considered as very reliable. Moreover, this also provides direct confidence in the kinetic frosting data presented in Fig. 3 for each separate fraction.

5. Conclusion

The frosting process of a glass in concentrated HF-based solutions is a delicate combination of both its dissolution and the gradual precipitation of a crust on its surface, resulting in a rather complicated macroscopic kinetics of the overall process. In this work, a decreasing etching rate with time was observed on four kinds of commercial glass substrates, both by chemical analysis of etched Si by ICP-OES and by glass weight loss measurements. Both independent methods also showed that increasing the HF concentration in the etching solution increased the initial etching rate in a non-linear way. Chemical analysis of Si by ICP-OES in the etching and frosting fractions revealed that increasing the HF concentration increased the amount of Si present in the crust. Also, for all HF concentrations, the initial etching rate increased with the amount of alumina in the glass, although the combined effect of oxides other than silica and alumina present in the glass could not be excluded.

The kinetics behind our experimental weight loss data was then quantified by a dissolution/precipitation model available in the literature. Moreover, we were able to extend its scope and obtain an independent estimation of both the relevant dissolution and deposition constants (K_{diss} and K_{dep}), respectively. Finally, we were also able to use these quantitative data to extract the surface density of the crust, and show how the latter varies as a function of glass composition and HF concentration.

References

[1] H. Totsuka, I. Sato, M. Anma, Suppression of haze formation on LCD glass and durability of the substrate etched by BHF, SID Symp. Dig. Tech. Pap. 31 (2000) 164–167.
[2] L. Wong, T. Suratwala, M.D. Feit, P.E. Miller, R. Steele, The effect of HF/NH_4F etching on the morphology of surface fractures on fused silica, J. Non-Cryst. Solids 355 (2009) 797–810.
[3] C. Iliescu, Wet etching of glass for MEMS applications, Rom. J. Inf. Sci. Technol. 9

(2006) 285–310.
[4] H. Nakanishi, T. Nishimoto, R. Nakamura, A. Yotsumoto, T. Yoshida, S. Shoji, Studies on SiO –SiO bonding with hydrofluoric acid. Room temperature and low stress bonding technique for MEMS, Sensors Actuators 79 (2000) 237–244.
[5] G.A.C.M. Spierings, Wet chemical etching of silicate glasses in hydrofluoric acid based solutions, J. Mater. Sci. 28 (1993) 6261–6273.
[6] C.D. Spencer, L. Ott, The frosting of glass by mixtures containing hydrofluoric acid and alkali fluorides, J. Am. Ceram. Soc. 10 (1927) 402–410.
[7] P. Barboux, A. Laghzizil, Y. Bessoles, H. Deroulhac, G. Trouvé, Paradoxical crystalline morphology of frosted glass, J. Non-Cryst. Solids 345–346 (2004) 137–141.
[8] J. Frayret, A. Castetbon, M. Potin-Gautier, M.F. Guimon, C. Guimon, Y. Bessoles, G. Trouvé, H. De Roulhac, A study of the process conditions that lead to an unusual frosted glass, Glass Technol. 46 (2005) 103–108.
[9] J.S. Judge, A study of the dissolution of SiO in acidic fluoride solutions, J. Electrochem. Soc. 118 (1971) 1772–1775.
[10] A. Mitra, J.D. Rimstidt, Solubility and dissolution rate of silica in acid fluoride solutions, Geochim. Cosmochim. Acta 73 (2009) 7045–7059.
[11] F.M. Ezz-Eldin, T.D. Abd-Elaziz, N.A. Elalaily, Effect of dilute HF solutions on chemical, optical, and mechanical properties of soda-lime-silica glass, J. Mater. Sci. 45 (2010) 5937–5949.
[12] G.A.C.M. Spierings, J. Van Dijk, The dissolution of Na2O-MgO-CaO-SiO2 glass in aqueous HF solutions, J. Mater. Sci. 22 (1987) 1869–1874.
[13] H. Kikyuama, N. Miki, K. Saka, J. Takano, I. Kawanabe, M. Miyashita, T. Ohmi, Principles of wet chemical processing in ULSI micro fabrication, IEEE Trans. Semicond. Manuf. 4 (1991) 26–35.
[14] D.J. Monk, D.S. Soane, R.T. Howe, A review of the chemical reaction mechanism and kinetics for hydrofluoric acid etching of silicon dioxide for surface micromachining applications, Thin Solid Films 232 (1993) 1–12.
[15] G.A.C.M. Spierings, Compositional effects in the dissolution of multicomponent silicate glasses in aqueous HF solutions, J. Mater. Sci. 26 (1991) 3329–3336.
[16] S. Verhaverbeke, I. Teerlinck, C. Vinckier, G. Stevens, R. Cartuyvels, M.M. Heyns, The etching mechanisms of SiO_2 in hydrofluoric acid, J. Electrochem. Soc. 141 (1994) 2852–2857.
[17] T. Hoshino, Y. Nishioka, Etching process of SiO_2 by HF molecules, J. Chem. Phys. 111 (1999) 2109–2114.
[18] D.M. Knotter, Etching mechanism of vitreous silicon dioxide in HF-based solutions, J. Am. Chem. Soc. 122 (2000) 4345–4351.
[19] J.K. Kang, C.B. Musgrave, The mechanism of HF/H_2O chemical etching of SiO_2, J. Chem. Phys. 116 (2002) 275–280.
[20] Y. Saito, S. Okamoto, H. Inomata, J. Kurachi, Mechanism of the etching rate change of aluminosilicate glass in HF acid with micro-indentation, Appl. Surf. Sci. 255 (2008) 2290–2294.
[21] Y. Saito, S. Okamoto, H. Inomata, J. Kurachi, T. Hidaka, H. Kasai, Micro-fabrication techniques applied to aluminosilicate glass surfaces: micro-indentation and wet etching process, Thin Solid Films 517 (2009) 2900–2904.
[22] J. Frayret, A. Castetbon, G. Trouvé, M. Potin-Gautier, Solubility of $(NH_4)_2SiF_6$, K_2SiF_6 and Na_2SiF_6 in acidic solutions, Chem. Phys. Lett. 427 (2006) 356–364.
[23] C. Iliescu, B. Chen, F.E.H. Tay, G. Xu, J. Miao, Characterization of deep wet etching of glass, PRO 6037, Device Process Technol. Microelectron. MEMS Photonics IV (2005) 1–12.
[24] C. Iliescu, B. Chen, J. Miao, On the wet etching of Pyrex glass, Sensors Actuators A 143 (2008) 154–161.
[25] G.M. Clarke, Statistics and Experimental Design, 2nd ed., Edward Arnold, 1980.